EVS32 Symposium
Lyon, France, May 19 - 22, 2019

Balanced model-order reduction technique of lithium-ion battery-cell internal electrochemical transfer functions

Albert Rodríguez[1,2], Gregory L. Plett[1], M. Scott Trimboli[1]
[1]*Department of Electrical and Computer Engineering, University of Colorado Colorado Springs, Colorado Springs, CO 80918, United States*
[2]*EURECAT - Technology Center of Catalonia, Barcelona, Spain*

Abstract

Electrochemical physics-based models are developed from the fundamental electromechanical equations that describe cell behavior (*i.e.*, full-order model) and therefore, allow detailed understanding of internal cell variables. The greatest challenge in using physics-based models stems from their computational complexity. To make a feasible physics-based model for battery management, we must construct reduced-order approximations of lithium-ion battery cell dynamics. We present a method to find a high-fidelity discrete-time state-space reduced-order model (ROM) that approximates infinite order transcendental electrochemical transfer functions of all electrochemical variables of interest.
Thus, for practical use, physics-based models based on infinite order transcendental electrochemical transfer functions need to be approximated using low-order models that capture their most significant dynamics. Here, we present the *Lagrange-interpolated realization algorithm* (LRA), which is a method that accurately approximates the actual continuous-time infinite-order electrochemical transfer function frequency response using a continuous-time high-order model (HOM). Then, the continuous-time HOM is discretized and reduced using balanced techniques, generating a reduced-order model (ROM) of order *n*.

Keywords: battery, lithium battery, battery model, BMS (Battery Management System).

1 Introduction

Electrochemical models are required to accurately describe all the important internal dynamics that occur when lithium-ion cells are being operated under different conditions. The full-order model of lithium-ion cells consists of four coupled partial differential equations and one algebraic equation. The partial differential equations that govern the full-order model arise from the fundamental principles of charge and mass conservation of the solid and electrolyte materials in the cell. The algebraic equation models the lithium flux from the solid to the electrolyte material. A set of full-order model (FOM) equations based on the original works [2, 3] describing lithium-ion cells having single-material negative and positive electrodes is thoroughly derived in [6]. Furthermore, lithium-ion cells having multiple-material electrodes are developed in [1].
The Doyle-Fuller-Newman (DFN) lithium-ion battery model is too complex to be used in an embedded battery-management system. To make a feasible physics-based model for battery management, various methods are proposed in the literature to construct reduced-order approximations of lithium-ion battery cell dynamics.

We prefer methods based on finding transfer functions of all electrochemical variables of interest and then converting these transfer functions into low-order high-fidelity discrete-time state-space approximate models. Physics-based models based on infinite order transcendental electrochemical transfer functions (*i.e.*, they cannot be expressed as a ratio of polynomials) are developed in [9, 5, 7]. Thus, for practical use, these systems need to be approximated using low-order models that capture their most significant dynamics. This paper proposes a novel model-order reduction technique whose objective is to generate reduced-order models from the infinite-order electrochemical transfer functions.
The technique presented will provide a reduced-order discrete-time state-space model of the form

$$x[k+1] = Ax[k] + Bu[k] \tag{1}$$

$$y[k] = Cx[k] + Du[k] \tag{2}$$

where the states of the system are represented by $x[k] \in \mathbb{R}^{n\times 1}$, the input by $u[k] \in \mathbb{R}^{m\times 1}$ and the output by $y[k] \in \mathbb{R}^{q\times 1}$. Note that *n* corresponds to the order of the model, *m* to the number of inputs and *q* to the number of outputs. Furthermore, the state-space matrices dimensions are $A \in \mathbb{R}^{n\times n}$, $B \in \mathbb{R}^{n\times m}$, $C \in \mathbb{R}^{q\times n}$ and the direct feed-through term $D \in \mathbb{R}^{q\times 1}$. The input $u[k]$ will correspond to the current applied to the cell (*i.e.*, $u[k] = i_{\text{app}}[k]$ and $m = 1$) and the linear outputs will correspond to the electrochemical variables of interest.

2 Solving for the state-space *A* matrix

In order to have consistent physics-based reduced-order models, state-space matrices are forced to have a certain structure. The state-space *A* matrix is diagonal, where the diagonal elements are sorted from smallest to largest and correspond to the eigenvalues of the system. Hence, the diagonal elements of *A* must be less than 1 in magnitude and be real for the discrete-time system to be stable and non oscillatory. That is,

$$A = \begin{bmatrix} a_1 & 0 & 0 & 0 & 0 \\ 0 & a_2 & 0 & 0 & 0 \\ 0 & 0 & \ddots & 0 & 0 \\ 0 & 0 & 0 & a_n & 0 \\ 0 & 0 & 0 & 0 & 1 \end{bmatrix}$$

where $|a_i| < 1 \; \forall \; i \in [1 \dots n]$ for a stable model, $a_i \in \mathbb{R} \; \forall \; i \in [1 \dots n]$ for a non-oscillatory system and $a_1 < a_2 < ... < a_n$. Notice that we add an integrator state (*i.e.*, unity eigenvalue) to be able to compute state-of-charge and also add any integrator pole transfer functions might have.
The *Lagrange-interpolated realization algorithm* (LRA) is a realization procedure that approximates the actual infinite-order transfer function frequency response using a continuous-time high-order model (HOM). The continuous-time HOM is discretized and reduced using balanced techniques, generating a reduced-order model (ROM) of order *n*.
A single-input single-output continuous-time rational transfer function of order $\bar{n}$ has the form

$$\overline{H}_q(s) = \frac{b_{\bar{n}-1}s^{\bar{n}-1} + \cdots + b_1 s + b_0}{s^{\bar{n}} + a_{\bar{n}-1}s^{\bar{n}-1} + \cdots + a_1 s + a_0} + d_0 \tag{3}$$

where d_0 corresponds to the direct feedthrough term and the coefficients a_i and b_i for $i \in [0 \dots \bar{n}-1]$ will determine the pole and zero locations of the transfer function. Notice we can accurately approximate any given transfer function $G_q(s)$ (even infinite-order transfer function) by using Lagrange interpolation. The Lagrange interpolation approach consists of estimating values between known data points. In frequency domain, we would like $\overline{H}_q(s) = G_q(s)$ at different frequency points s_i. That is, $\overline{H}_q(s_i) = G_q(s_i)$ for $i \in [1 \dots \bar{n}]$ where $\bar{n}$ corresponds to the transfer function order. Note that we have $2\bar{n}$ degrees of freedom corresponding to the number of *a* and *b* coefficients to be estimated. However, we only use $\bar{n}$ different frequency points in order to obtain real valued coefficients since the other $\bar{n}$ points will correspond to their negative frequencies, that is, $\overline{H}_q(s_i) = G_q(s_i)$ and $\overline{H}_q(-s_i) = G_q(-s_i)$. Therefore, we need to solve a $2\bar{n}$ system of equations to determine the coefficients a and b from Eq. (3). The system of

equations to be solved looks like

$$
\begin{aligned}
G_q(s_1) &= \frac{b_{\bar{n}-1}s_1^{\bar{n}-1} + \cdots + b_1 s_1 + b_0}{s_1^{\bar{n}} + a_{\bar{n}-1}s_1^{\bar{n}-1} + \cdots + a_1 s_1 + a_0} + d_0 \\
G_q(-s_1) &= \frac{b_{\bar{n}-1}(-s_1)^{\bar{n}-1} + \cdots + b_1(-s_1) + b_0}{(-s_1)^{\bar{n}} + a_{\bar{n}-1}(-s_1)^{\bar{n}-1} + \cdots + a_1(-s_1) + a_0} + d_0 \\
G_q(s_2) &= \frac{b_{\bar{n}-1}s_2^{\bar{n}-1} + \cdots + b_1 s_2 + b_0}{s_2^{\bar{n}} + a_{\bar{n}-1}s_2^{\bar{n}-1} + \cdots + a_1 s_2 + a_0} + d_0 \\
G_q(-s_2) &= \frac{b_{\bar{n}-1}(-s_2)^{\bar{n}-1} + \cdots + b_1(-s_2) + b_0}{(-s_2)^{\bar{n}} + a_{\bar{n}-1}(-s_2)^{\bar{n}-1} + \cdots + a_1(-s_2) + a_0} + d_0 \\
&\vdots \\
G_q(s_{\bar{n}}) &= \frac{b_{\bar{n}-1}s_{\bar{n}}^{\bar{n}-1} + \cdots + b_1 s_{\bar{n}} + b_0}{s_{\bar{n}}^{\bar{n}} + a_{\bar{n}-1}s_{\bar{n}}^{\bar{n}-1} + \cdots + a_1 s_{\bar{n}} + a_0} + d_0 \\
G_q(-s_{\bar{n}}) &= \frac{b_{\bar{n}-1}(-s_{\bar{n}})^{\bar{n}-1} + \cdots + b_1(-s_{\bar{n}}) + b_0}{(-s_{\bar{n}})^{\bar{n}} + a_{\bar{n}-1}(-s_{\bar{n}})^{\bar{n}-1} + \cdots + a_1(-s_{\bar{n}}) + a_0} + d_0
\end{aligned}
$$

where large order $\bar{n}$ will produce a very accurate approximation of $G_q(s)$. However, as $\bar{n}$ increases, the computational requirements to solve the linear[1] system of equations also increase.

Once we have obtained a high-order continuous-time rational transfer function $\overline{H}_q(s)$ that accurately approximates the true (infinite-order) frequency response, we can easily convert it to state-space representation (*e.g.*, using `tf2ss.m` in Matlab), that is, $\overline{H}_q(s) = \overline{C}_q(sI_{\bar{n}} - \overline{A}_q)\overline{B}_q + \overline{D}_q$. Further, for our application, we expect $\overline{A}_q$ to have real, stable poles, which is not guaranteed by the method as presented so far. So, we elect to replace unstable poles in $\overline{A}_q$ by their reciprocals (maintaining the magnitude response) and complex poles by their magnitudes (largely maintaining the magnitude response). In addition, we set $\overline{B}_q = 1_{n\times 1}$ and we also re-compute the state-space $\overline{C}_q$ matrix using the method described in Section 4.

Notice that the approach explained above is valid for SISO systems only and therefore, need to be extended to SIMO systems. Since we are only interested in a high-order approximation (*i.e.*, we do not care about the model order), we can easily extend the approach to the SIMO case by assembling the different SISO high-order models. That is,

$$
\overline{A} = \begin{bmatrix} \overline{A}_1 & 0 & 0 & 0 \\ 0 & \overline{A}_2 & 0 & 0 \\ 0 & 0 & \ddots & 0 \\ 0 & 0 & 0 & \overline{A}_q \end{bmatrix}, \qquad \overline{B} = \begin{bmatrix} \overline{B}_1 \\ \overline{B}_2 \\ \vdots \\ \overline{B}_q \end{bmatrix}, \tag{4}
$$

$$
\overline{C} = \begin{bmatrix} \overline{C}_1 & 0 & \dots & 0 \\ 0 & \overline{C}_2 & 0 & 0 \\ 0 & 0 & \ddots & 0 \\ 0 & 0 & 0 & \overline{C}_q \end{bmatrix}, \qquad \overline{D} = \begin{bmatrix} \overline{D}_1 \\ \overline{D}_2 \\ \vdots \\ \overline{D}_q \end{bmatrix}, \tag{5}
$$

where the state-space matrices $\overline{A}_q$, $\overline{B}_q$, $\overline{C}_q$ and $\overline{D}_q$ correspond to the continuous-time HOM approximation the transfer function *q*. Thus, the $\overline{A}$, $\overline{B}$, $\overline{C}$ and $\overline{D}$ matrices estimate a total of *q* continuous-time transfer functions. Then, the continuous-time state-space model can be discretized with a given sampling

[1] Notice that $G_q(s_i) = \frac{b_{\bar{n}-1}s_i^{\bar{n}-1}+\cdots+b_1 s_i+b_0}{s_i^{\bar{n}}+a_{\bar{n}-1}s_i^{\bar{n}-1}+\cdots+a_1 s_i+a_0} + d_0$ can be written as $(G_q(s_i) - d_0)\left(s_i^{\bar{n}} + a_{\bar{n}-1}s_i^{\bar{n}-1} + \cdots + a_1 s_i + a_0\right) = b_{\bar{n}-1}s_i^{\bar{n}-1} + \cdots + b_1 s_i + b_0$

time T_s by computing the discrete-time state-space matrices as

$$\overline{A}_d = \exp\left(\overline{A}T_s\right) \tag{6}$$

$$\overline{B}_d = \overline{A}^{-1}(\overline{A}_d - I_{\bar{n}})\overline{B} \tag{7}$$

$$\overline{C}_d = \overline{C} \tag{8}$$

$$\overline{D}_d = \overline{D} \tag{9}$$

where the subscript *d* refers to discrete-time matrices and $\overline{H}(z) = \overline{C}_d(zI_{\bar{n}} - \overline{A}_d)\overline{B}_d + \overline{D}_d$.
The next step is to perform a balanced model order reduction [10] to the discrete-time high-order model $\overline{H}(z)$ in order to obtain the final discrete-time reduced-order model *A* matrix of a given order *n*.
To summarize the LRA method:

1. Approximate the actual continuous-time frequency response $G_q(s)$ using a rational continuous-time high-order model $\overline{H}_q(s)$ via solving $G_q(s_i) = \overline{H}_q(s_i)$ and $G_q(-s_i) = \overline{H}_q(-s_i)$ for $i \in [1 \ldots \bar{n}]$.
2. Repeat Step 1 for each transfer function to be estimated. Then, assemble the individual high-order models via Eqs. (4) and (5) to build $\overline{H}(s)$. Further, replace unstable poles in $\overline{A}$ by their reciprocals (maintaining the magnitude response) and complex poles by their magnitudes (largely maintaining the magnitude response). In addition, set $\overline{B} = 1_{n\times 1}$ and re-compute the state-space $\overline{C}$ matrix using the method described in Section 4.
3. Discretize the rational high-order model $\overline{H}(s)$ to obtain a discrete-time high-order model $\overline{H}(z)$ via Eqs. (6) to (9).
4. Perform a balanced realization of the discrete-time HOM $\overline{H}(z)$ to obtain the discrete-time state-space *A* matrix.

3 Solving for the state-space *B* matrix

The *B* matrix is forced to be a column vector of ones. That is,

$$B = \begin{bmatrix}1 & 1 & \ldots & 1 & 1\end{bmatrix}^T$$

4 Solving for the state-space *C* matrix

The structure of the output matrix *C*, which determines the contribution of each of the states to the output is

$$C = \begin{bmatrix} c_{11} & c_{12} & \cdots & c_{1n} & \text{res}_1^* \\ c_{21} & c_{22} & \cdots & c_{2n} & \text{res}_2^* \\ \vdots & \vdots & \ddots & \vdots & \vdots \\ c_{q1} & c_{q2} & \cdots & c_{qn} & \text{res}_q^* \end{bmatrix} \tag{10}$$

where *q* corresponds to the number of outputs, or in other words, the number of electrochemical transfer functions to be estimated, *n* corresponds to the model order and res* corresponds to the residue of the integrator pole, which is computed as

$$\text{res}^* = \lim_{s\to 0} sG(s).$$

Then, electrochemical transfer functions with integrator pole can be expressed as:

$$[G(s)]^* = G(s) - \text{res}^*/s$$

where $[G(s)]^*$ corresponds to the electrochemical transfer function with the integrator pole removed, $G(s)$ corresponds to the original transfer function and res^*/s corresponds to the integrator pole. Notice that $\text{res}^* = 0$ if the original transfer function does not have any integrator pole.
This section introduces an optimal approach to solve for the *C* state-space matrix using least squares that ensures the dc gain of the reduced-order model agrees with the actual dc gain of the transfer functions. Recall that the *B* matrix is a column vector of ones as described in Section 3 and the *D* matrix can be found analytically as explained in Section 5.
When solving for the *C* matrix, we desire to minimize the squares of the errors between the actual and approximate frequency responses while enforcing that the dc gain of the approximated system exactly matches the dc gain of the actual system. To do so, we formulate a constrained optimization cost function to be minimized as

$$J = \sum_{k=1}^{N} \|G(\omega_k) - H(\omega_k)\|_2^2 + \lambda^T \left(G(0) - H(0)\right)$$

where G corresponds to the actual frequency response and H corresponds to the low-order approximation of G. For simplicity, we compute $G(\omega_k) = G(e^{j\omega_k T_s}) - D$ and $H(\omega_k) = C(e^{j\omega_k T_s} I - A)^{-1} B$. Let $M(\omega_k) = (e^{j\omega_k T_s} I - A)^{-1} B$; then, $H(\omega_k) = CM(\omega_k)$ and

$$\begin{aligned} J &= \left\{ \sum_{k=1}^{N} \left[G(\omega_k) - H(\omega_k)\right]^* \left[G(\omega_k) - H(\omega_k)\right] \right\} \\ &\quad + \lambda^T \left(G(0) - H(0)\right) \\ &= \left\{ \sum_{k=1}^{N} \text{Tr}\left[G^*(\omega_k) G(\omega_k)\right] - \text{Tr}\left[G(\omega_k) M^*(\omega_k) C^T\right] \right. \\ &\quad \left. - \text{Tr}\left[CM(\omega_k) G^*(\omega_k)\right] + \text{Tr}\left[CM(\omega_k) M^*(\omega_k) C^T\right] \right\} \\ &\quad + \text{Tr}\left[\left(G(0) - CM(0)\right) \lambda^T\right]. \end{aligned}$$

Taking derivatives of J with respect to λ and C gives

$$\begin{aligned} \frac{\partial J}{\partial \lambda} &= G(0) - CM(0) = 0 \\ \frac{\partial J}{\partial C^T} &= -2 \underbrace{\sum_{k=1}^{N} \mathbb{R}\left[G(\omega_k) M^*(\omega_k)\right]}_{M_1} + 2C \underbrace{\sum_{k=1}^{N} \mathbb{R}\left[M(\omega_k) M^*(\omega_k)\right]}_{M_2} \\ &\quad - \lambda M^T(0) = 0. \end{aligned}$$

Transposing and combining into one matrix equation, we solve the following for *C* using least squares. That is,

$$\begin{bmatrix} 2M_2^T & -M(0) \\ M^T(0) & 0 \end{bmatrix} \begin{bmatrix} C^T \\ \lambda^T \end{bmatrix} = \begin{bmatrix} 2M_1^T \\ G^T(0) \end{bmatrix}. \tag{11}$$

In summary, using the approach presented in this section, we can compute the *C* matrix that minimizes the squares of the errors between the actual and approximated frequency responses while enforcing that the dc gain of the approximated system exactly matches the dc gain of the actual system.
Notice that we need to augment the obtained *C* matrix in order to add back the integrator residues as seen in Eq. (10).

5 Solving for the state-space *D* matrix

The *D* matrix (or the direct feedthrough term) models the instantaneous change in output $y[k]$ when the system is excited with input $u[k]$. In this case, the *D* matrix can be found in closed-form since the electrochemical transfer functions are analytical. That is,

$$D = \left[\lim_{s\to\infty} G_1(s),\ \lim_{s\to\infty} G_2(s),\ \ldots,\ \lim_{s\to\infty} G_q(s)\right]^T. \tag{12}$$

6 Results

This section presents the performance of the *Lagrange-interpolated realization algorithm* (LRA). The discrete-time reduced-order models generated using the LRA have been assumed to have order $n = 6$ and $T_s = 1\,\text{s}$. In addition, the examples shown estimate a total of 21 transfer functions, corresponding to:

$$\begin{aligned}
[\widetilde{C}_{s,e}(\bar{x},z)]^*/I_{\text{app}}(z) \quad & \text{at } \bar{x} = [0,1,2,3] \\
J(\bar{x},z)/I_{\text{app}}(z) \quad & \text{at } \bar{x} = [0,1,2,3] \\
[\widetilde{\Phi}_{s,e}(\bar{x},z)]^*/I_{\text{app}}(z) \quad & \text{at } \bar{x} = [0,1,2,3] \\
\widetilde{\Phi}_{e}(\bar{x},z)/I_{\text{app}}(z) \quad & \text{at } \bar{x} = [1,2,3] \\
\widetilde{\Phi}_{s}(\bar{x},z)/I_{\text{app}}(z) \quad & \text{at } \bar{x} = [1,2] \\
\widetilde{C}_{e}(\bar{x},z)/I_{\text{app}}(z) \quad & \text{at } \bar{x} = [0,1,2,3]
\end{aligned}$$

where $\bar{x} = 0$ corresponds to the negative-electroce current collector, $\bar{x} = 1$ to the negative-electrode/separator boundary, $\bar{x} = 2$ to the separator/positive-electrode boundary and $\bar{x} = 3$ to the positive-electrode current collector. The structure of these electrochemical transfer functions are shown in [8] and the cell parameters used are listed in Table 1 in the Appendix.
Recall that since reduced-order models provide the linear estimates of the electrochemical variables, nonlinear corrections need to be added back to the linear outputs. That is,

- The linear output of the reduced-order model $j^{\text{r}}(\bar{x},t)$ is the approximation to the true reaction flux. That is, no additional correction is needed.
- The solid-surface concentration estimate is computed by adding the initial solid concentration $c^{\text{r}}_{s,0}$ to the linear output $\tilde{c}^{\text{r}}_{s,e}(\bar{x},t)$. That is, $c^{\text{r}}_{s,e}(\bar{x},t) = \tilde{c}^{\text{r}}_{s,e}(\bar{x},t) + c^{\text{r}}_{s,0}$.
- The phase-potential difference variable can be computed as $\phi^{\text{r}}_{s\text{-}e}(\bar{x},t) = \tilde{\phi}^{\text{r,*}}_{s\text{-}e}(\bar{x},t) + U^{\text{n}}_{\text{ocp}}(c^{\text{n}}_{s,\text{avg}}(t))$ where $\tilde{\phi}^{\text{r,*}}_{s\text{-}e}(\bar{x},t)$ refers to the linear output of the phase-potential difference variable with the integrator dynamics removed and $c^{\text{n}}_{s,\text{avg}}(t)$ corresponds to the negative-electrode average solid concentration.
- In the negative-electrode, $\phi^{\text{n}}_s(0,t) = 0$, because it is our reference and therefore, $\phi^{\text{p}}_s(0,t) = v_{\text{cell}}$. Hence, $\phi^{\text{n}}_s(\bar{x},t)$ corresponds to the linear output of the state-space model, and $\phi^{\text{p}}_s(\bar{x},t) = \tilde{\phi}^{\text{p}}_s(\bar{x},t) + v_{\text{cell}}(t)$, where $\tilde{\phi}^{\text{p}}_s(\bar{x},t)$ also corresponds to the linear output of the solid potential.
- The electrolyte potential variable is computed as $\phi^{\text{r}}_e(\bar{x},t) = \tilde{\phi}^{\text{r}}_e(\bar{x},t) - \tilde{\phi}^{\text{n,*}}_{s\text{-}e}(0,t) - U^{\text{n}}_{\text{ocp}}(c^{\text{n}}_{s,\text{avg}}(t))$ where $\tilde{\phi}^{\text{r}}_e(\bar{x},t)$ corresponds to the linear output of the electrolyte potential, $\tilde{\phi}^{\text{n,*}}_{s\text{-}e}(\bar{x},t)$ refers to the linear output of the negative-electrode phase-potential difference variable with the integrator dynamics removed and $c^{\text{n}}_{s,\text{avg}}(t)$ corresponds to the negative-electrode average solid concentration.
- The actual electrolyte concentration estimate is computed as $c^{\text{r}}_e(\bar{x},t) = \tilde{c}^{\text{r}}_e(\bar{x},t) + c_{e,0}$ where $c_{e,0}$ corresponds to the initial electrolyte concentration and $\tilde{c}^{\text{r}}_e(\bar{x},t)$ corresponds to the linear output of the electrolyte concentration.
- The voltage of the cell is computed by combining different electrochemical variables. That is,

$$\begin{aligned}
v_{\text{cell}}(t) = {} & (\eta^{\text{p}}(0,t) - \eta^{\text{n}}(0,t)) + (\phi^{\text{p}}_e(0,t) - \phi^{\text{n}}_e(0,t)) \\
& + \left(U^{\text{p}}_{\text{ocp}}(0,t) - U^{\text{n}}_{\text{ocp}}(0,t)\right) + F\left(R^{\text{p}}_{\text{film}} j^{\text{p}}(0,t) - R^{\text{n}}_{\text{film}} j^{\text{n}}(0,t)\right)
\end{aligned} \tag{13}$$

  where if we assume that the charge-transfer coefficient $\alpha = 0.5$, as is often the case, we can write the overpotential $\eta^{\text{r}}(\bar{x},t)$ as

$$\eta^{\text{r}}(\bar{x},t) = \frac{2RT}{F}\text{asinh}\left(\frac{j^{\text{r}}(\bar{x},t)}{2k^{\text{r}}_0\sqrt{c^{\text{r}}_e(\bar{x},t)\left(c^{\text{r}}_{s,\max} - c^{\text{r}}_{s,e}(\bar{x},t)\right)c^{\text{r}}_{s,e}(\bar{x},t)}}\right).$$

The performance[2] of the *Lagrange-interpolated realization algorithm* (LRA) is addressed in this section;

[2] Computational performance was not the principal focus of this work and therefore, the code is not optimized.

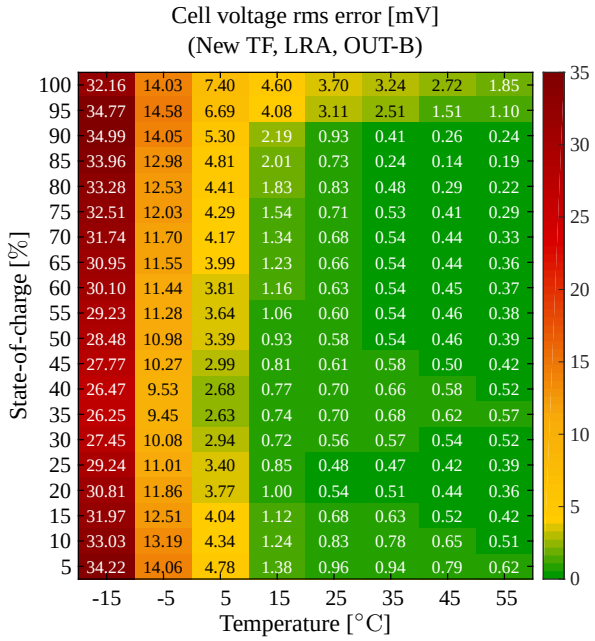

Figure 1: Performance of LRA using *new* electrochemical transfer functions.

that is, speed, memory, robustness and accuracy. It is also worth mentioning that the overall performance of the LRA depends on its tuning parameters. The results shown correspond to the following set of tuning parameters:

- The continuous-time frequency vector for building $G(s)$ was chosen to comprise one point at $\omega = 0$, 30 additional points spaced evenly on a logarithmic scale between 10^{-12} and 10^{-6} (to capture very slow dynamics) and 500 additional points spaced evenly on a logarithmic scale between 10^{-6} and 10^{7} (to capture the rest of dynamics).
- The order of each transfer function to be estimated was chosen to be $\bar{n}_i = 40$ for $i \in [1 \dots q]$. Hence, the order of the complete high-order system is $\bar{n} = \bar{n}_i q$ where q corresponds to the total number of transfer functions to be estimated.

Speed: The LRA average run time is 66.00 seconds where most of the time is used to solve the linear system of equations.

Memory: The largest matrix size used by LRA is 5.645 MB, which corresponds to the high-order model A matrix. The A matrix dimension is $\bar{n} = \bar{n}_i q$ where $\bar{n}_i$ is the order of each transfer function to be estimated and q corresponds to the total number of transfer functions to be estimated. Notice that if we generate reduced-order models from $-15°\mathrm{C}$ to $55\mathrm{C}$ in $10°\mathrm{C}$ increments and from 0% to 100% state-of-charge in 5% increments, we would need a total of 168 models, which would take approximately 3 hours.

Robustness: The LRA is enforced to produce real and stable poles by replacing unstable poles in A by their reciprocals (maintaining the magnitude response) and complex poles by their magnitudes (largely maintaining the magnitude response).

Accuracy: We are most interested in the time-domain performance of physics-based reduced-order models generated using the LRA. Figure 1 shows the cell voltage root-mean squared error between the full-order model and the physics-based reduced-order model generated using the *Lagrange-interpolated realization algorithm* for a 3-min 0.5C constant-current discharge pulse followed by a 2-min rest period starting at different state-of-charge and temperatures. The smallest cell voltage root-mean squared error is 0.14 mV corresponding to 85% state-of-charge and $45°\mathrm{C}$.
Figure 2 shows the frequency domain performance of the LRA when approximating the phase potential difference transfer function at the cell boundaries. We see that the reduced order model generated using the LRA approach is in complete agreement with the actual transfer function. Recall that the actual transfer function has an infinite number of poles and zeros and the reduced-order model is approximating a total of 21 transfer functions using only 6 poles.

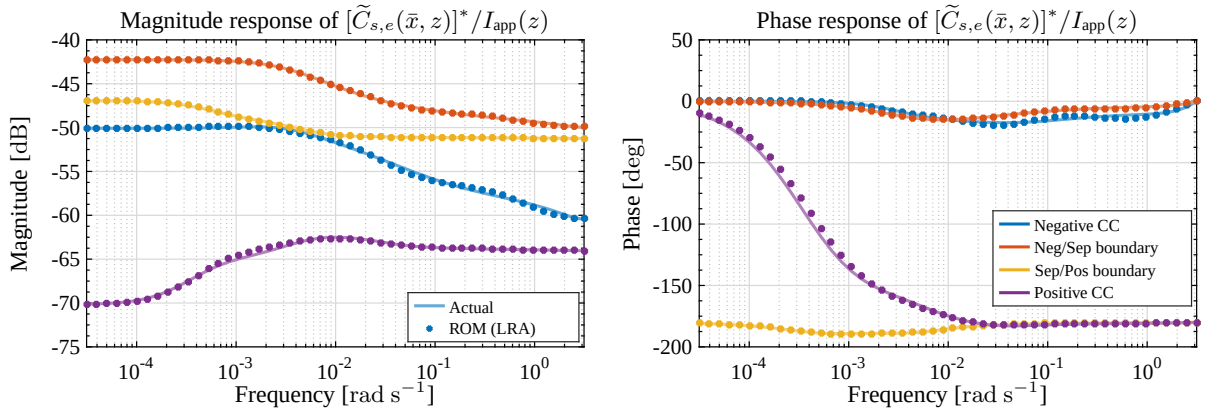

Figure 2: Performance of the LRA approximating $[\widetilde{\Phi}_{s,e}(\bar{x},z)]^*/I_{\text{app}}(z)$ at $\bar{x} = [0, 1, 2, 3]$.

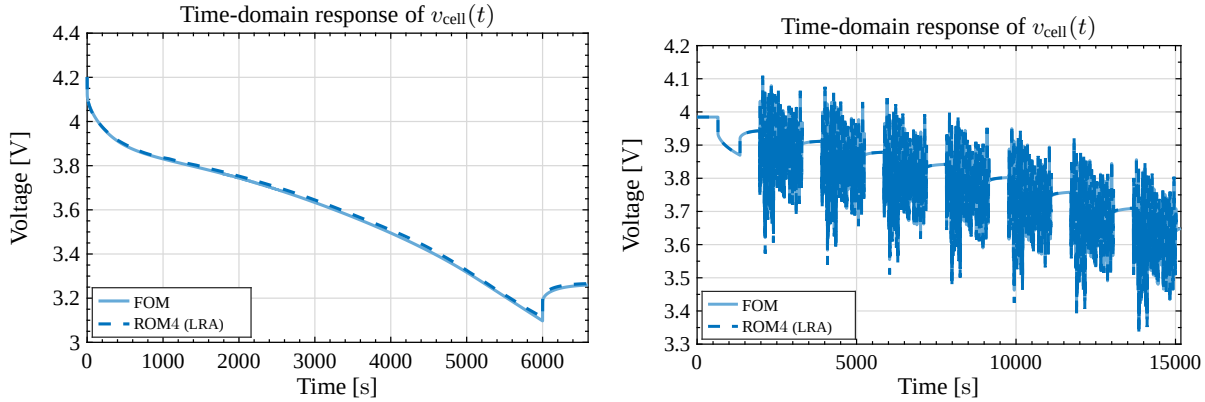

Figure 3: $v_{\text{cell}}(t)$ simulation result using LRA to generate the ROMs.

In order to verify how the good frequency response approximation of the LRA translates into good time domain results, cell voltage $v_{\text{cell}}(t)$ for 7 consecutive UDDS cycles and a long 0.5C constant-current discharge is shown in Fig. 3. The agreement between the full-order model and the (4th order) physics-based reduced-order model is outstanding. We see cell voltage is accurately predicted for high dynamic simulations and also long constant-current events. The root-mean squared error between the full-order model and the reduced-order model generated using the *Lagrange-interpolated realization algorithm* is 3.18 mV for the 7 consecutive UDDS cycles and 9.88 mV for the long 0.5C constant-current discharge.

Acknowledgement

The information, data, or work presented herein was funded in part by General Motors as part of the "Physics-based reduced-order model for vehicle BSE" project. This work used the EAS Data Center or EAS Cloud, which is supported by the College of Engineering and Applied Science at the University of Colorado Colorado Springs. The authors would like to express their gratitude to each of these sponsors.

References

[1] Paul Albertus, Jake Christensen, and John Newman. Experiments on and modeling of positive electrodes with multiple active materials for lithium-ion batteries. *Journal of The Electrochemical Society*, 156(7):A606–A618, 2009.

[2] Marc Doyle, Thomas F. Fuller, and John Newman. Modeling of galvanostatic charge and discharge of the lithium/polymer/insertion cell. *Journal of the Electrochemical Society*, 140(6):1526–1533, June 1993.

[3] Thomas F. Fuller, Marc Doyle, and John Newman. Simulation and optimization of the dual lithium ion insertion cell. *Journal of the Electrochemical Society*, 141(1):1–10, January 1994.

[4] W. Gu and C. Wang. Thermal-electrochemical coupled modeling of a lithium-ion cell.

[5] James L. Lee, Andrew Chemistruck, and Gregory L. Plett. One-dimensional physics-based reduced-order model of lithium-ion dynamics. *Journal of Power Sources*, 220(0):430 – 448, 2012.

[6] Gregory L. Plett. *Battery Management Systems: Volume 1, Battery Modeling*. Artech House, 2015.

[7] Albert Rodríguez and Gregory L. Plett. Controls-oriented models of lithium-ion cells having blend electrodes. part 2: Physics-based reduced-order models. *Journal of Energy Storage*, 11(Supplement C):219 – 236, 2017.

[8] Albert Rodríguez, Gregory L. Plett, and M. Scott Trimboli. Improved transfer functions modeling linearized lithium-ion battery-cell internal electrochemical variables. *Journal of Energy Storage*, 20:560 – 575, 2018.

[9] Kandler A. Smith. *Electrochemical Modeling, Estimation and Control of Lithium Ion Batteries*. PhD thesis, Pennsylvania State University, 2006.

[10] A. Varga. Balancing free square-root algorithm for computing singular perturbation approximations. In *Proceedings of the 30th IEEE Conference on Decision and Control*, volume 2, pages 1062–1065, Dec 1991.

Authors

Albert Rodríguez was born in Barcelona, Spain, in 1991. He received his B.Eng. degree in energy engineering from the Polytechnic University of Catalonia, Spain, in 2013 and the M.Sc. and Ph.D. degrees in electrical engineering from the University of Colorado Colorado Springs, United States, in 2015 and 2017, respectively. He joined EURECAT, the Technologic Centre of Catalonia, as head of the battery research group in 2018. His current research focuses on identification, modeling, simulation, testing and control of battery systems including physics-based reduced-order modeling of lithium-ion dynamics, state-of-charge and state-of-health estimation, cell internal state estimation and control-systems theory as applied to the management of high-capacity battery systems.

Professor Plett received his Ph.D. in Electrical Engineering from Stanford University in 1998. Since then, he has been on the faculty of the Department of Electrical and Computer Engineering at the University of Colorado Colorado Springs. His research focuses on control-systems theory as applied to the management of high-capacity battery systems, such as found in hybrid and electric vehicles. Current research efforts include: physics-based reduced-order modeling of ideal lithium-ion dynamics; system identification of physics-based model parameters using only current-voltage input-output data; physics-based reduced-order modeling of degradation mechanisms in electrochemical cells; estimation of cell internal state and degradation state; state-of-charge, state-of-health and state-of-life estimation; power and energy prediction; and battery pack fast charging.

Associate Professor Trimboli received his Ph.D. in Control Engineering from University of Oxford in 1989. He joined the faculty of the University of Colorado Colorado Springs in 2011, where his research focuses on development of control strategies for the management of high-capacity battery systems such as found in electric vehicles. He is currently UCCS principal investigator (PI) of a multi-year program with the Office of Naval Research (ONR) headed by Utah State University where he leads a team investigating the application of model-predictive control to improve the performance and extend the lifetime of lithium ion battery cells. Other research efforts include: physics-based reduced-order modeling of ideal lithium-ion dynamics, physics-based modeling of lithium-ion degradation dynamics, empirical and physics-based modeling of lithium-ion thermal dynamics, as well as predictive methods for power estimation.

A Cell parameters

The parameters of the cell listed in Table 1 are used in this publication and were those published by Lee *et al.* [5], except for the activation energies, which were extracted from [4].

Table 1: Cell parameters for simulation.

Symbol	Units	Negative electrode	Separator	Positive electrode
L	μm	128	76	190
R_s	μm	12.5	-	8.5
A	m^2	1	1	1
σ	$\mathrm{S\,m^{-1}}$	100	-	3.8
E_a^σ	$\mathrm{kJ\,mol^{-1}}$	0	-	0
ε_s	$\mathrm{m^3 m^{-3}}$	0.471	-	0.297
ε_e	$\mathrm{m^3 m^{-3}}$	0.357	0.724	0.444
brug	-	1.5	-	1.5
$c_{s,\max}$	$\mathrm{mol\,m^{-3}}$	26 390	-	22 860
$c_{e,0}$	$\mathrm{mol\,m^{-3}}$	2000	2000	2000
θ_0	-	0.05	-	0.78
θ_{100}	-	0.53	-	0.17
D_s	$\mathrm{m^2\,s^{-1}}$	3.9×10^{-14}	-	1.0×10^{-13}
$E_a^{D_s}$	$\mathrm{kJ\,mol^{-1}}$	4	-	20
D_e	$\mathrm{m^2\,s^{-1}}$	7.5×10^{-11}	7.5×10^{-11}	7.5×10^{-11}
$E_a^{D_e}$	$\mathrm{kJ\,mol^{-1}}$	10	10	10
E_a^κ	$\mathrm{kJ\,mol^{-1}}$	20	20	20
t_+^0	-	0.363	0.363	0.363
k_0	$\mathrm{mol\,m^{-2}\,s^{-1}}$	2.29×10^{-5}	-	2.21×10^{-5}
$E_a^{k_0}$	$\mathrm{kJ\,mol^{-1}}$	30	-	30
α	-	0.5	-	0.5
R_{film}	$\Omega\,\mathrm{m^2}$	0.0	-	0.0
$\mathrm{d}\ln f_\pm / \mathrm{d}\ln c_e$	-	3	3	3

We compute $\sigma^{\text{eff}} = \sigma\varepsilon_s$, $\kappa^{\text{eff}} = \kappa\varepsilon_e^{\text{brug}}$, $D_e^{\text{eff}} = D_e\varepsilon_e^{\text{brug}}$.
In the electrolyte, conductivity is a function of concentration:

$$\begin{aligned}\kappa(c_e) &= 4.1253 \times 10^{-2} + 5.007 \times 10^{-4} c_e - 4.7212 \times 10^{-7} c_e^2 \\ &\quad + 1.5094 \times 10^{-10} c_e^3 - 1.6018 \times 10^{-14} c_e^4.\end{aligned}$$

For the negative electrode, the open-circuit potential function is:

$$U_{\text{ocp}}(\theta) = -0.16 + 1.32\exp\left(-3.0\theta\right) + 10.0\exp\left(-2000.0\theta\right).$$

For the positive electrode, the open-circuit potential function is:

$$\begin{aligned}U_{\text{ocp}}(\theta) &= 4.19829 + 0.0565661\tanh\left(-14.5546\theta + 8.60942\right) \\ &\quad -0.0275479\left[\frac{1}{(0.998432-\theta)^{0.492465}} - 1.90111\right] \\ &\quad -0.157123\exp(-0.04738\theta^8) + 0.810239\exp\left[-40(\theta - 0.133875)\right].\end{aligned}$$